nature immunology

The kinase Jnk2 promotes stress-induced mitophagy by targeting the small mitochondrial form of the tumor suppressor ARF for degradation

Qiao Zhang[1,2,5], Hong Kuang[1,2,5], Cong Chen[1], Jie Yan[3], Hanh Chi Do-Umehara[1], Xin-yuan Liu[2], Laura Dada[1], Karen M Ridge[1,4], Navdeep S Chandel[1] & Jing Liu[1]

Mitophagy is essential for cellular homeostasis, but how mitophagy is regulated is largely unknown. Here we found that the kinase Jnk2 was required for stress-induced mitophagy. Jnk2 promoted ubiquitination and proteasomal degradation of the small mitochondrial form of the tumor suppressor ARF (smARF). Loss of Jnk2 led to the accumulation of smARF, which induced excessive autophagy that resulted in lysosomal degradation of the mitophagy adaptor p62 at steady state. Depletion of p62 prevented Jnk2-deficient cells from mounting mitophagy upon stress. Jnk2-deficient mice displayed defective mitophagy, which resulted in tissue damage under hypoxic stress, as well as hyperactivation of inflammasomes and increased mortality in sepsis. Our findings define a unique mechanism of maintaining immunological homeostasis that protects the host from tissue damage and mortality.

Mitophagy, a selective form of autophagy that removes damaged or excessive mitochondria, is essential for maintaining cellular energy homeostasis and functions[1,2]. Deregulation of mitophagy has been linked to many pathophysiological activities and diseases[1,2]. Accumulating evidence suggests that mitophagy has a crucial role in the regulation of immune responses[3–5]. Defects in the clearance of damaged mitochondria by mitophagy result in the production of excessive reactive oxygen species (ROS) and damage-associated molecular patterns, which leads to hyperactivation of the NLRP3 inflammasome, which can induce tissue and organ damage and increased mortality in the host[3–5].

The mitophagy machinery has been investigated extensively, but details of the mechanism by which it acts are still largely unclear. A prominent theme is that the E3 ubiquitin ligase parkin and the kinase PINK1 ('tumor suppressor PTEN–induced putative kinase 1') mediate the priming of damaged mitochondria for mitophagy[6–9]. PINK1 is constitutively degraded in healthy mitochondria but is stabilized on the outer membrane of damaged mitochondria, where it recruits and activates parkin by phosphorylating Ser65 of parkin[6–9]. Activated parkin ubiquitinates mitochondrial substrates, which in turn trigger translocation of the ubiquitin and autophagy markers and LC3–binding adaptors p62 (sequestosome-1 (SQSTM1)) or NBR1 to damaged mitochondria for the subsequent formation of autophagosome that will fuse with the lysosome (autolysosome) for degradation[1,2,6,8,10–16]. p62 itself is degraded together with enveloped cytosolic contents in the autolysosome during autophagy and mitophagy and thus serves as a marker of autophagy, but its abundance is restored at later phase of autophagy and mitophagy through transcriptional upregulation[17,18].

Small mitochondrial ARF (smARF) is a short isoform of the tumor suppressor ARF produced by alternative translational initiation at Met45; it localizes exclusively to mitochondria[19,20]. The abundance of smARF in steady-state conditions is extremely low due to constant degradation by the proteasome[19–21]. Analyses using ectopic expression approaches have reported that overexpression of smARF is able to induce mitochondrial depolarization and subsequent autophagy and mitophagy[19,20,22]. However, the pathophysiological function and regulation of endogenous smARF is not known.

The Jnk ('c-Jun amino-terminal kinase'; stress-activated protein kinase (SAPK))[23] kinases are a subfamily of the mitogen-activated protein kinase superfamily. Jnk is involved in the regulation of many cellular activities, from gene expression to apoptosis[23–25]. Jnk has two ubiquitously expressed isoforms, Jnk1 and Jnk2, which share 83% amino acid identity and have shared and distinct functions[23–25]. Jnk1 is the main isoform of Jnk that is activated by a variety of extracellular stimuli, whereas Jnk2 activity is negligible[26]. Instead, in unstimulated cells, Jnk2 targets its substrates, including c-Jun, ATF-2 and p53, for proteasomal degradation independently of its kinase activity[27–31]. It has been reported that Jnk1, but not Jnk2, contributes to starvation-induced autophagy by phosphorylating the antiapoptotic protein Bcl-2, which leads to its dissociation from the autophagy protein beclin-1 (ref. 32). However, it is not known whether these two Jnk isoforms regulate mitophagy. Here we found that Jnk2 promoted

[1]Division of Pulmonary and Critical Care Medicine, Feinberg School of Medicine, Northwestern University, Chicago, Illinois, USA. [2]State Xinyuan Institute of Medicine and Biotechnology, College of Life Science, Zhejiang Sci-Tech University, Hangzhou, China. [3]Ben May Department for Cancer Research, The University of Chicago, Chicago, Illinois, USA. [4]Jesse Brown Veterans Affairs Medical Center, Chicago, Illinois, USA. [5]These authors contributed equally to this work. Correspondence should be addressed to J.L. (jing@northwestern.edu).

Received 17 November 2014; accepted 19 February 2015; published online 23 March 2015; doi:10.1038/ni.3130

ubiquitination-dependent proteasomal degradation of endogenous smARF, which otherwise triggered lysosomal degradation of p62 through augmentation of steady-state autophagy. Jnk2-deficient mice displayed defective mitophagy, which resulted in tissue damage under hypoxic stress and hyperactivation of inflammasomes and increased mortality during sepsis.

RESULTS

Stress-induced mitophagy requires Jnk2

To understand the role of Jnk in regulation of stress-induced mitophagy, we used Jnk1- or Jnk2-deficient mouse embryonic fibroblasts (MEFs). Immunoblot analysis showed that mitochondrial proteins (Tom20 for the outer membrane; TIM23 and/or ATP5β for the inner membrane; and cytochrome C and/or hsp60 for mitochondrial matrix) were much less abundant in wild-type fibroblasts cultured under hypoxic conditions or treated with the protonophore CCCP (carbonyl cyanide m-chlorophenyl hydrazone) or starved by incubation in HBSS (Hank's balanced salt solution) than in wild-type cells cultured in complete growth medium under normoxic conditions (without CCCP treatment) (**Fig. 1a**,**b** and **Supplementary Fig. 1a**), consistent with published reports[33–36]. The decrease was caused by mitophagy, as it was prevented by bafilomycin A1, a lysosomal inhibitor of ATPase (**Supplementary Fig. 1b**,**c**). Under the same conditions, the decrease in mitochondrial proteins was inhibited in Jnk2-deficient (*Mapk9*$^{-/-}$; called '*Jnk2*$^{-/-}$' here) MEFs but not in Jnk1-deficient (*Mapk8*$^{-/-}$; called '*Jnk1*$^{-/-}$' here) MEFs (**Fig. 1a**,**b** and **Supplementary Fig. 1d**–**g**). The ratio of punctation with green fluorescent protein (GFP)-tagged LC3 that localized with mitochondria was significantly lower in *Jnk2*$^{-/-}$ MEFs than in wild-type fibroblasts (**Fig. 1c**,**d**). We also demonstrated defects in mitochondrial clearance in *Jnk2*$^{-/-}$ cells by immunofluorescence microscopy with antibody to Tom20 (anti-Tom20) (**Fig. 1e**,**f**) and transmission electron microscopy (**Fig. 1g**). Ectopic expression of hemagglutinin (HA)-tagged Jnk2 restored mitophagy in *Jnk2*$^{-/-}$ MEFs (**Supplementary Fig. 1h**–**j**), which suggested that the loss of Jnk2, rather than other genetic alterations, was responsible for the defective mitophagy. Furthermore, *Jnk2*$^{-/-}$ MEFs produced excessive mitochondrial ROS (**Fig. 1h**), indicative of the accumulation of damaged mitochondria. Notably, the general autophagy activity induced by hypoxia or HBSS was not altered by loss of Jnk2, as indicated by formation of the lipidated form of LC3 (LC3(II)) (**Supplementary Fig. 1k**). Together these data suggested that Jnk2 was required for stress-induced mitophagy.

Jnk2 is essential for maintaining p62 abundance at steady state

The initiation of mitophagy is mediated by the stabilization of PINK1 and translocation of parkin to the mitochondrial outer membrane[6–9]. We assessed these two events in wild-type and *Jnk2*$^{-/-}$ MEFs under hypoxic conditions or following treatment with CCCP. There were no substantial differences between wild-type MEFs and *Jnk2*$^{-/-}$ MEFs under either condition in their stabilization of PINK1 (**Supplementary Fig. 2a**,**b**) or recruitment of parkin to mitochondria (**Supplementary Fig. 2c**). p62 is specifically needed to mediate mitophagy but is dispensable for general autophagy[1,2,6,8,10–17]. We sought to determine whether Jnk2 might regulate mitophagy by affecting p62 expression. As expected, expression of p62 was much lower in wild-type fibroblasts under hypoxic conditions than in normoxia and was much lower after stimulation with CCCP or

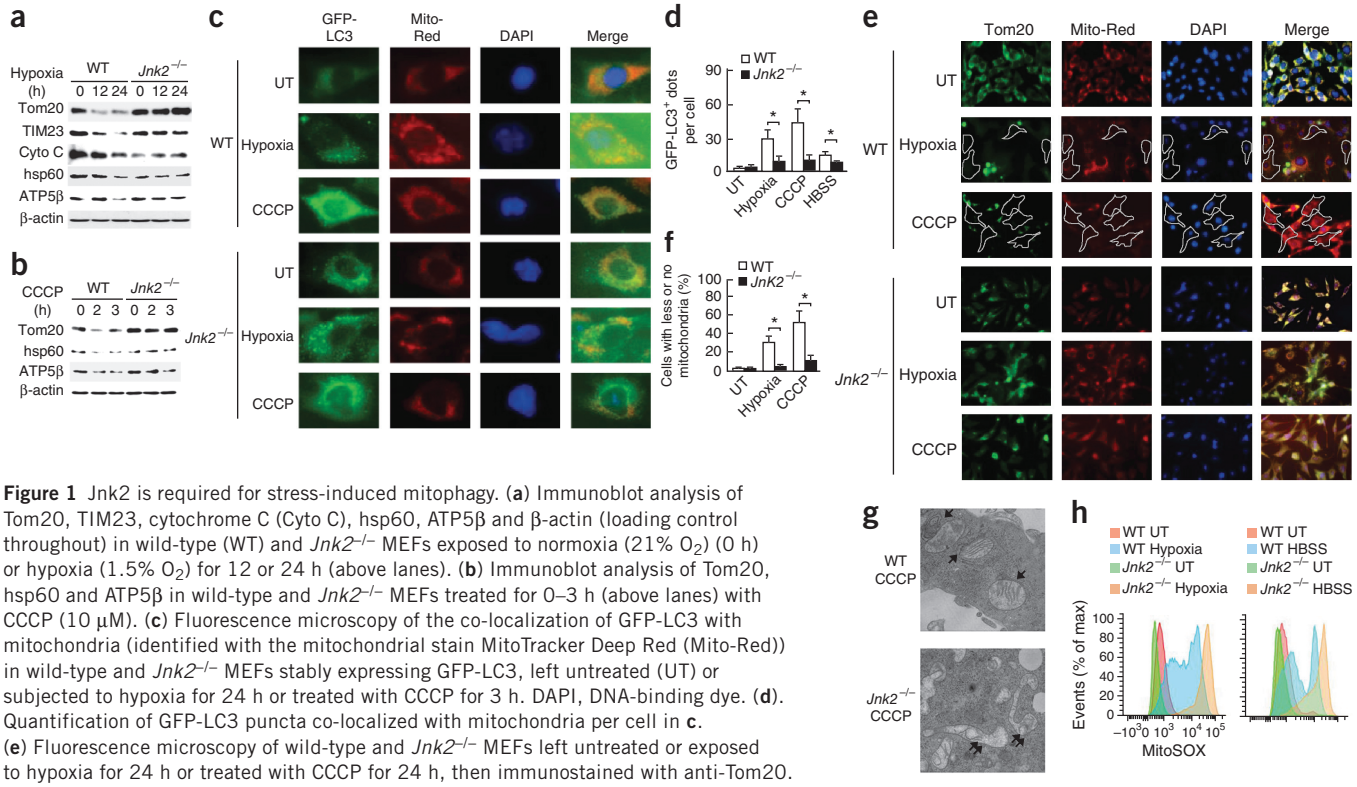

Figure 1 Jnk2 is required for stress-induced mitophagy. (**a**) Immunoblot analysis of Tom20, TIM23, cytochrome C (Cyto C), hsp60, ATP5β and β-actin (loading control throughout) in wild-type (WT) and *Jnk2*$^{-/-}$ MEFs exposed to normoxia (21% O_2) (0 h) or hypoxia (1.5% O_2) for 12 or 24 h (above lanes). (**b**) Immunoblot analysis of Tom20, hsp60 and ATP5β in wild-type and *Jnk2*$^{-/-}$ MEFs treated for 0–3 h (above lanes) with CCCP (10 μM). (**c**) Fluorescence microscopy of the co-localization of GFP-LC3 with mitochondria (identified with the mitochondrial stain MitoTracker Deep Red (Mito-Red)) in wild-type and *Jnk2*$^{-/-}$ MEFs stably expressing GFP-LC3, left untreated (UT) or subjected to hypoxia for 24 h or treated with CCCP for 3 h. DAPI, DNA-binding dye. (**d**) Quantification of GFP-LC3 puncta co-localized with mitochondria per cell in **c**. (**e**) Fluorescence microscopy of wild-type and *Jnk2*$^{-/-}$ MEFs left untreated or exposed to hypoxia for 24 h or treated with CCCP for 24 h, then immunostained with anti-Tom20. (**f**) Frequency of cells in **e** with fewer mitochondria than untreated wild-type MEFs or no mitochondria. (**g**) Transmission electron microscopy of wild-type and *Jnk2*$^{-/-}$ MEFs treated for 24 h with CCCP: arrows indicate engulfed mitochondria in autophagosomes; double arrows indicate swollen mitochondria with disrupted cristae. (**h**) Flow cytometry of wild-type and *Jnk2*$^{-/-}$ MEFs left untreated or subjected to hypoxia or treated with HBSS, then stained with MitoSOX (a fluorogenic dye targeted to mitochondria that produces red fluorescence after oxidation by superoxide). Original magnification, ×40 (**c**,**e**,**f**). *$P < 0.05$ (unpaired Student's *t*-test). Data are representative of at least three independent experiments (mean and s.e.m. of 100 cells (**d**) or 20 individual fields (**f**)).

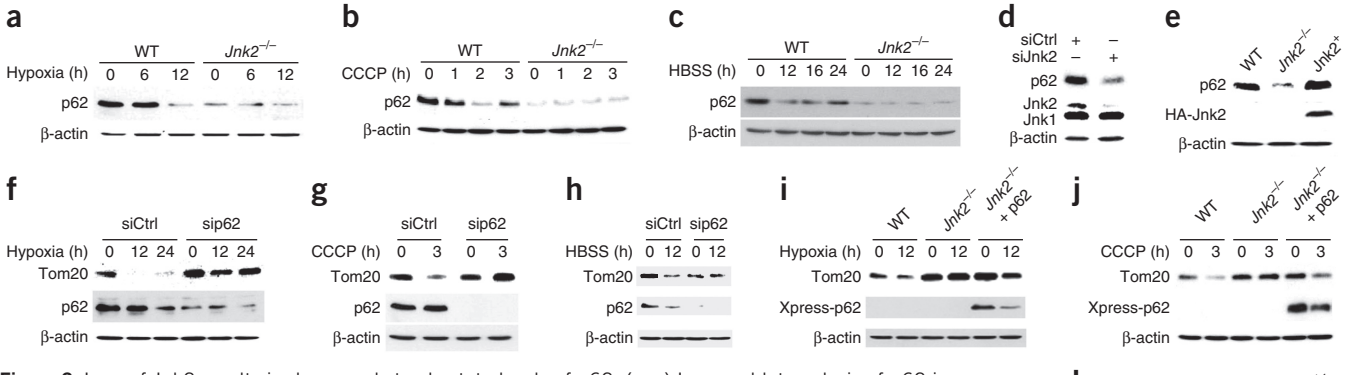

Figure 2 Loss of Jnk2 results in decreased steady-state levels of p62. (**a**–**c**) Immunoblot analysis of p62 in wild-type and *Jnk2*$^{-/-}$ MEFs treated for various times (above lanes) with hypoxia (**a**), CCCP (**b**) or HBSS (**c**). (**d**) Immunoblot analysis of p62, Jnk2 and Jnk1 in wild-type MEFs transfected with nontargeting control siRNA (siCtrl) or *Jnk2*-specific siRNA (siJnk2). (**e**) Immunoblot analysis of p62 and HA-Jnk2 in wild-type MEFs transfected with empty vector (WT) or in *Jnk2*$^{-/-}$ MEFs 48 h after transfection of empty vector (*Jnk2*$^{-/-}$) or expression vector encoding HA-Jnk2 (Jnk2^{+}). (**f**–**h**) Immunoblot analysis of Tom20 and p62 in wild-type MEFs transfected with control siRNA (siCtrl) or siRNA targeting mRNA encoding p62 (sip62), then, 36 h later, treated for various times (above lanes) with hypoxia (**f**), CCCP (**g**) or HBSS (**h**). (**i**–**k**) Immunoblot analysis of Tom20 and Xpress-tagged p62 in wild-type MEFs transfected with empty vector (WT) or *Jnk2*$^{-/-}$ MEFs transfected with empty vector (*Jnk2*$^{-/-}$) or with expression vector encoding Xpress-tagged p62 (*Jnk2*$^{-/-}$ + p62), then, 36 h later, treated for various times (above lanes) with hypoxia (**i**), CCCP (**j**) or HBSS (**k**). Data are representative of three independent experiments.

HBSS than before such stimulation (**Fig. 2a**–**c**), consistent with published reports that p62 is degraded together with enveloped cytosolic contents in the autolysosome during autophagy[17]. Notably, the steady-state abundance of p62 was considerably lower in *Jnk2*$^{-/-}$ MEFs than in wild-type MEFs (**Fig. 2a**–**c**). We obtained similar results when we silenced *Jnk2* through the use of *Jnk2*-specific small interfering RNA (siRNA) (**Fig. 2d**). Conversely, ectopic expression of HA-Jnk2 restored the steady-state abundance of p62 in *Jnk2*$^{-/-}$ MEFs (**Fig. 2e**). Under our experimental conditions, p62 was required for mitophagy induced by hypoxia, CCCP or HBSS, as indicated by the observation that silencing of the gene encoding p62 significantly inhibited the degradation of Tom20 in response to hypoxia, CCCP or HBSS (**Fig. 2f**–**h**). More notably, ectopic expression of Xpress-tagged p62 restored the degradation of Tom20 in *Jnk2*$^{-/-}$ MEFs in response to hypoxia, CCCP or HBSS (**Fig. 2i**–**k**). Thus, these data demonstrated that loss of Jnk2 substantially diminished the steady-state abundance of p62, which resulted in defective mitophagy upon stress.

Jnk2 suppresses excessive autophagy at steady state

p62 is degraded together with enveloped cytosolic contents in the autolysosome during the induction of autophagy and thus serves as

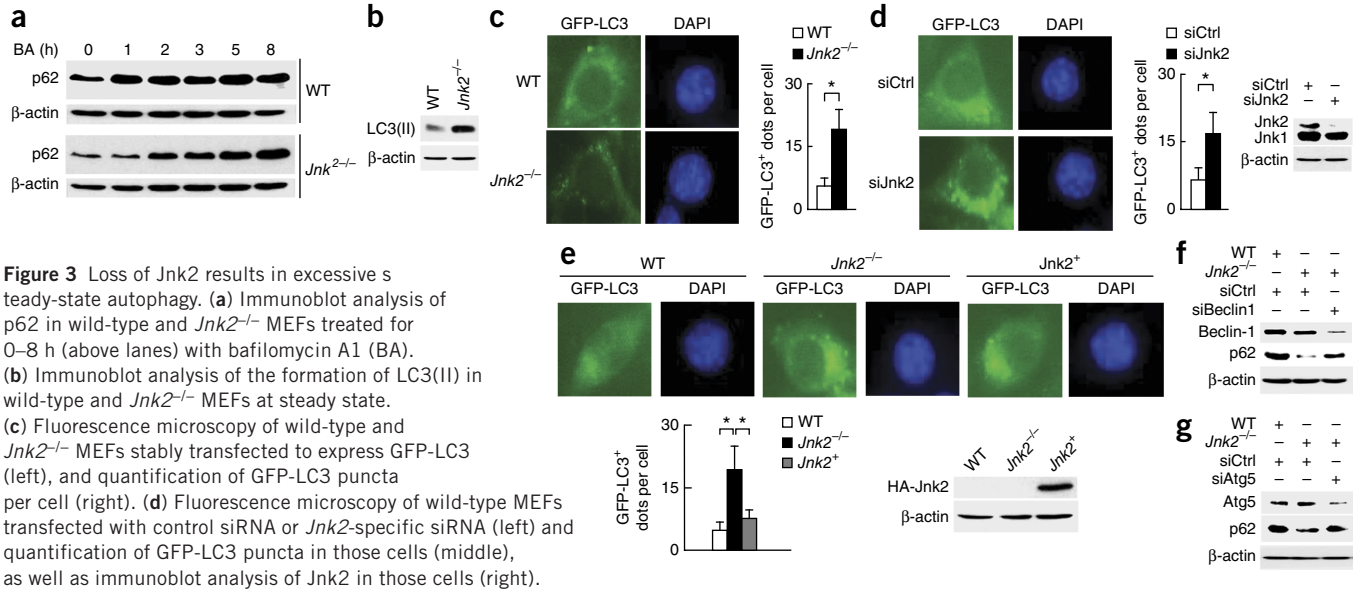

Figure 3 Loss of Jnk2 results in excessive s teady-state autophagy. (**a**) Immunoblot analysis of p62 in wild-type and *Jnk2*$^{-/-}$ MEFs treated for 0–8 h (above lanes) with bafilomycin A1 (BA). (**b**) Immunoblot analysis of the formation of LC3(II) in wild-type and *Jnk2*$^{-/-}$ MEFs at steady state. (**c**) Fluorescence microscopy of wild-type and *Jnk2*$^{-/-}$ MEFs stably transfected to express GFP-LC3 (left), and quantification of GFP-LC3 puncta per cell (right). (**d**) Fluorescence microscopy of wild-type MEFs transfected with control siRNA or *Jnk2*-specific siRNA (left) and quantification of GFP-LC3 puncta in those cells (middle), as well as immunoblot analysis of Jnk2 in those cells (right). (**e**) Fluorescence microscopy of wild-type MEFs stably expressing GFP-LC3, transfected with empty vector (WT), or *Jnk2*$^{-/-}$ MEFs stably expressing GFP-LC3, transfected with empty vector (*Jnk2*$^{-/-}$) or expression vector encoding HA-Jnk2 (Jnk2^{+}) (top), and quantification of GFP-LC3 puncta in those cells (bottom left), as well as immunoblot analysis of HA-Jnk2 in those cells (bottom right). (**f**,**g**) Immunoblot analysis of beclin-1 and p62 (**f**) or Atg5 and p62 (**g**) in *Jnk2*$^{-/-}$ MEFs transfected with control siRNA or siRNA targeting the gene encoding beclin-1 (siBeclin1) (**f**) or Atg5 (siAtg5) (**g**). Original magnification, ×40 (**c**,**d**,**e**). *$P < 0.05$ (unpaired Student's *t*-test). Data are representative of three independent experiments (mean and s.e.m. of 100 cells in **c**–**e**).

a marker of autophagy. The steady-state abundance of p62 is strictly regulated by degradation via steady-state autophagy[1,2,16,20,22–29,37]. We investigated whether loss of Jnk2 triggered more autophagy during basal conditions to enhance the degradation of steady-state p62, which would result in subsequently defective mitophagy upon stress. Real-time RT-PCR revealed that the abundance of p62 mRNA was similar in wild-type and *Jnk2*$^{-/-}$ fibroblasts (**Supplementary Fig. 3**). However, treatment of *Jnk2*$^{-/-}$ MEFs with bafilomycin A1 led to accumulation of p62 to amounts similar to those in wild-type fibroblasts cultured under similar conditions (**Fig. 3a**); this indicated enhanced lysosomal degradation of p62 in the absence of Jnk2. Consistent with that, LC3(II) formation and GFP-LC3 punctation were greater in *Jnk2*$^{-/-}$ MEFs than in wild-type fibroblasts under unstimulated conditions (**Fig. 3b**,**c**). We obtained similar results when we silenced *Jnk2* through the use of *Jnk2*-specific siRNA (**Fig. 3d**). Ectopic expression of HA-Jnk2 in *Jnk2*$^{-/-}$ MEFs diminished the steady-state autophagy to a level similar to that observed in wild-type fibroblasts (**Fig. 3e**). Furthermore, silencing of genes encoding the essential autophagy-associated molecules beclin-1 or Atg5 restored p62 protein expression in *Jnk2*$^{-/-}$ MEFs (**Fig. 3f**,**g**). These data together suggested that the enhanced steady-state autophagy in *Jnk2*$^{-/-}$ MEFs was responsible for the lower steady-state expression of p62, which prevented these cells from mounting efficient mitophagy upon stress.

Loss of Jnk2 stabilizes smARF

The enhanced steady-state autophagy in *Jnk2*$^{-/-}$ MEFs might have resulted from increased expression of genes encoding pro-autophagy molecules, such as beclin-1 or Atg5. This possibility was not the case, since there was no detectable difference between wild-type and *Jnk2*$^{-/-}$ fibroblasts in their abundance of beclin-1 or Atg5 protein (**Supplementary Fig. 4a**). It has been reported that overexpression of smARF potently induces autophagy and mitophagy[19]. We found that expression of smARF protein was barely detectable in wild-type fibroblasts (**Fig. 4a**), consistent with published reports that smARF is quickly turned over through proteasomal degradation at steady state[19]. In contrast, the abundance of smARF protein was much greater in *Jnk2*$^{-/-}$ MEFs than in wild-type MEFs at steady state (**Fig. 4a**). We confirmed the identity of smARF in *Jnk2*$^{-/-}$ MEFs by several approaches. First, two siRNAs targeting different positions on mRNA encoding ARF were able to reduce the expression of both full-length ARF (p19ARF) and smARF in *Jnk2*$^{-/-}$ MEFs (**Supplementary Fig. 4b**). Second, immunoblot analysis with an antibody that recognizes an epitope in the carboxyl terminus of ARF different from the epitope recognized by the anti-ARF used in our other studies also revealed more abundance of smARF in *Jnk2*$^{-/-}$ MEFs (**Supplementary Fig. 4c**). Finally, mass spectrometry of smARF proteins immunoprecipitated from *Jnk2*$^{-/-}$ MEFs recovered a peptide with the sequence LPGHAGGAAR, which is part of p19ARF

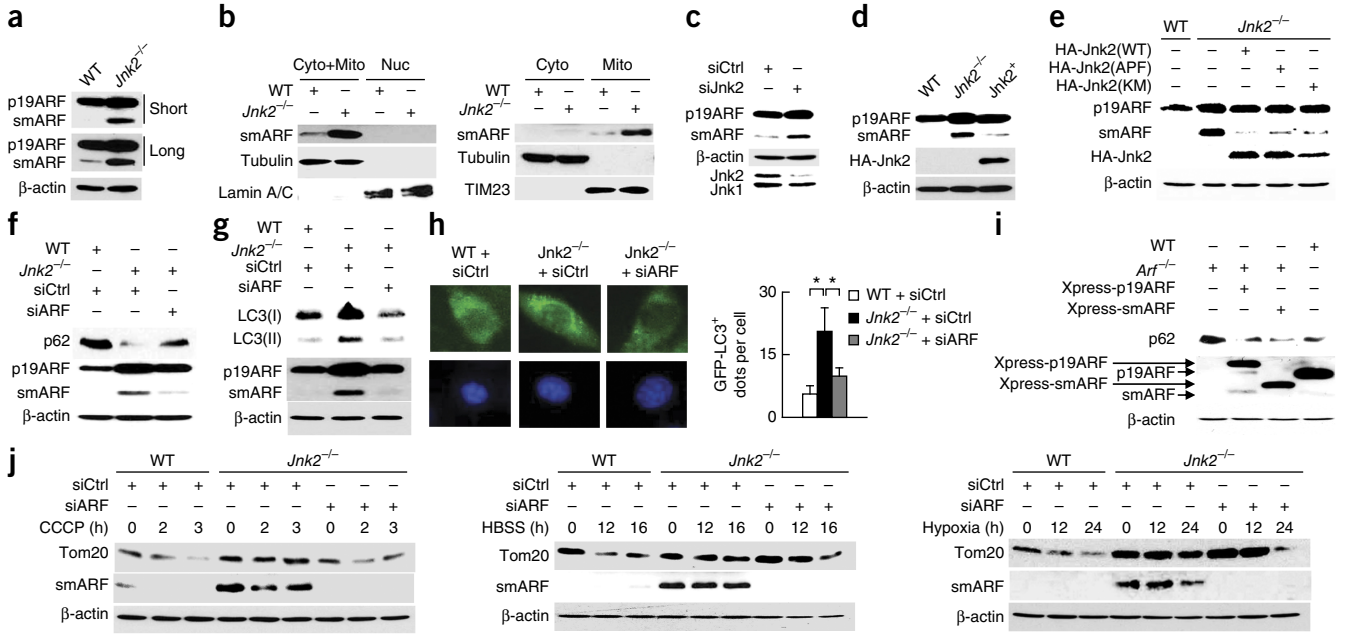

Figure 4 Loss of Jnk2 stabilizes smARF. (**a**) Immunoblot analysis of p19ARF and smARF wild-type and *Jnk2*$^{-/-}$ MEFs, probed with antibody to ARF that recognizes both full-length p19ARF and smARF (right margin, exposure time). (**b**) Immunoblot analysis of smARF, tubulin (cytoplasmic marker), lamin A/C (nuclear marker) and TIM23 (mitochondrial marker) in wild-type and *Jnk2*$^{-/-}$ MEFs fractionated into cytosolic plus mitochondrial (Cyto + Mito), nuclear (Nuc), cytosolic (Cyto) or mitochondrial (Mito) fractions. (**c**) Immunoblot analysis of p19ARF, smARF, Jnk1 and Jnk2 in wild-type MEFs transfected with control or *Jnk2*-secific siRNA. (**d**) Immunoblot analysis of p19ARF, smARF and HA-Jnk2 in wild-type MEFs transfected with empty vector (WT) and in *Jnk2*$^{-/-}$ MEFs transfected with empty vector (*Jnk2*$^{-/-}$) or with expression vector encoding HA-Jnk2 (Jnk2^{+}). (**e**) Immunoblot analysis of p19ARF, smARF and HA-Jnk2 in wild-type and *Jnk2*$^{-/-}$ MEFs transfected with empty vector (–) or to express (+) HA-tagged wild-type Jnk2 (HA-Jnk2(WT)) or the Jnk2 kinase activity–deficient mutants Jnk2(APF) or Jnk2(KM). (**f**) Immunoblot analysis of p62, p19ARF and smARF in wild-type and *Jnk2*$^{-/-}$ MEFs transfected with control or *Arf*-specific siRNA. (**g**) Immunoblot analysis of cytosolic LC3 (LC3(I)) and the formation of LC3(II), as well as p19ARF and smARF, in wild-type and *Jnk2*$^{-/-}$ MEFs transfected with control or *Arf*-specific siRNA (siARF). (**h**) Fluorescence microscopy of wild-type and *Jnk2*$^{-/-}$ MEFs transfected with siRNA as in **g** (left), and quantification of GFP-LC3 puncta per cell (right). Original magnification, ×40 (left). (**i**) Immunoblot analysis of p62, p19ARF and smARF in wild-type and *Arf*$^{-/-}$ MEFs transfected with empty vector or with expression vector encoding Xpress-tagged p19ARF or Xpress-tagged smARF. (**j**) Immunoblot analysis of Tom20 and smARF in wild-type or *Jnk2*$^{-/-}$ MEFs transfected with control or *Arf*-specific siRNA, and, 36 h later, treated for various times (above lanes) with CCCP, HBSS or hypoxia. **P* < 0.05 (unpaired Student's *t*-test). Data are representative of at least three independent experiments (mean and s.e.m. of 100 cells in **h**).

and smARF (**Supplementary Fig. 4d**). The accumulated smARF was targeted exclusively to the mitochondria in *Jnk2*$^{-/-}$ MEFs (**Fig. 4b**), consistent with published reports showing that smARF is localized to mitochondria[19]. We obtained similar results by silencing *Jnk2*, but not by silencing *Jnk1* (**Fig. 4c** and **Supplementary Fig. 4e**). Silencing of *Jnk2* also enhanced the abundance of exogenous Xpress-tagged smARF (**Supplementary Fig. 4f**). Conversely, expression of exogenous HA-Jnk2 substantially diminished the abundance of smARF protein in *Jnk2*$^{-/-}$ MEFs (**Fig. 4d**).

Next we investigated whether the kinase activity of Jnk2 was required for its regulation of smARF. Like the expression of wild-type Jnk2, the expression of either of two kinase activity–deficient mutants of Jnk2 reduced the amount of smARF protein in *Jnk2*$^{-/-}$ MEFs (**Fig. 4e**), which suggested that the kinase activity of Jnk2 was not required for its regulation of smARF expression. Jnk1 activity is enhanced in unstimulated *Jnk2*$^{-/-}$ MEFs[26]. It is plausible that the accumulated smARF proteins in *Jnk2*$^{-/-}$ MEFs were the result of increased Jnk1 activity. However silencing of *Jnk1* in *Jnk2*$^{-/-}$ MEFs did not affect the expression of smARF protein (**Supplementary Fig. 4g**). Thus, the enzymatic activity of Jnk was not involved in regulating the stability of smARF protein.

To determine whether increased abundance of smARF was responsible for the enhanced degradation of steady-state p62 in *Jnk2*$^{-/-}$ MEFs, we silenced the gene encoding ARF (*Cdkn2a*; called '*Arf*' here) in *Jnk2*$^{-/-}$ MEFs. Since smARF is the product of alternative translational initiation of ARF, *Arf*-specific siRNA will affect both full-length p19ARF and smARF. To avoid the influence of *Arf*-specific siRNA on the expression of full-length p19ARF, we transfected *Jnk2*$^{-/-}$ MEFs with *Arf*-specific siRNA at a relatively low dose (20 nM) that substantially decreased the expression of smARF but not of full-length p19ARF (**Fig. 4f,g**). Under these conditions, p62 protein was stabilized (**Fig. 4f**), while the enhanced formation of LC3(II) and GFP-LC3 punctation was diminished in *Jnk2*$^{-/-}$ MEFs (**Fig. 4g,h**). Thus, smARF may have accounted for the greater autophagy activity and lower p62 abundance in *Jnk2*$^{-/-}$ MEFs at steady state. In further support of that notion, expression of p62 protein was higher in *Arf*$^{-/-}$ MEFs than in wild-type MEFs but was diminished to amounts similar to those of wild-type MEFs in *Arf*$^{-/-}$ MEFs transfected with either an expression vector encoding p19ARF, which generated full-length p19ARF and smARF, or an expression vector encoding smARF (**Fig. 4i**). However, complementation of *Arf*$^{-/-}$ cells with mutant ARF in which the methionine at position 45 was replaced with isoleucine, and thus only full-length p19ARF was generated, did not diminish the steady-state abundance of p62 (**Supplementary Fig. 4h**). Furthermore, transfection with *Arf*-specific siRNA at a low dose that substantially decreased the expression of smARF but not of full-length p19ARF restored mitophagy in *Jnk2*$^{-/-}$ MEFs in response to hypoxia, CCCP or HBSS (**Fig. 4j**). Finally, in *Arf*$^{-/-}$ MEFs, the steady-state expression of p62 and stress-induced mitophagy were not affected by silencing of *Jnk2* (**Supplementary Fig. 4i**). Together these data suggested that stabilization of smARF in the absence of Jnk2 was mainly responsible for the excessive autophagy and subsequently lysosomal degradation of p62 at steady state, which led to defective mitophagy under stress.

Jnk2 promotes ubiquitination and degradation of smARF

The steady-state expression of smARF was extremely low in wild-type fibroblasts and became detectable only when cells were treated with the proteasome inhibitor MG-132, but not when they were treated with bafilomycin A1 (**Fig. 5a** and **Supplementary Fig. 5a**), consistent with a published report showing that smARF is rapidly degraded by the proteasome in unstimulated cells[19]. In contrast, MG-132 was unable to further increase the abundance of smARF protein in *Jnk2*$^{-/-}$ MEFs (**Fig. 5a**). This finding was not the result of defect in proteasome activity in *Jnk2*$^{-/-}$ fibroblasts, as shown by the abundance of the hypoxia-inducible factor HIF-1α before and after hypoxia treatment, as well as degradation of the inhibitor IκBα induced by tumor-necrosis factor (**Supplementary Fig. 5b,c**). The half-life of smARF was much greater in *Jnk2*$^{-/-}$ MEFs than in wild-type fibroblasts (**Fig. 5b**), and the rapid turnover of smARF in wild-type fibroblasts was inhibited by MG-132 (**Fig. 5c**). These data suggested that Jnk2 promoted the proteasomal degradation of steady-state smARF.

To determine whether Jnk2 triggered the ubiquitination-dependent proteasomal degradation of smARF, we generated wild-type fibroblasts that stably expressed Xpress-tagged smARF and transfected the cells with *Jnk2*-specific siRNA or nontargeting (control) siRNA. We analyzed ubiquitination of Xpress-tagged smARF by immunoprecipitation with antibody to the Xpress tag, followed by immunoblot analysis with antibody to total ubiquitin or the antibody to Lys48 (K48) linkage–specific ubiquitin. Silencing of *Jnk2* significantly

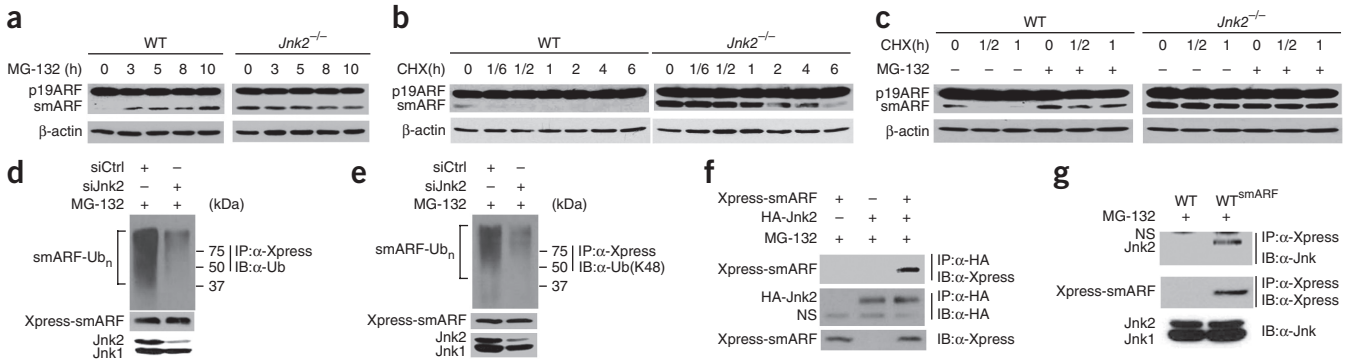

Figure 5 Jnk2 promotes the ubiquitination and degradation of smARF. (**a**,**b**) Immunoblot analysis of p19ARF and smARF in wild-type and *Jnk2*$^{-/-}$ MEFs treated for various times (above lanes) with MG-132 (**a**) or cycloheximide (CHX) (**b**). (**c**) Immunoblot analysis of p19ARF and smARF in wild-type and *Jnk2*$^{-/-}$ MEFs treated for 0–1 h (above lanes) with cycloheximide in the presence (+) or absence (–) of MG-132. (**d**,**e**) Immunoassay of the ubiquitination of smARF (smARF-Ub$_n$) in wild-type MEFs stably expressing Xpress-tagged smARF, transfected with control or *Jnk2*-specific siRNA, followed by immunoprecipitation (IP) with anti-Xpress (α-Xpress) and immunoblot analysis (IB) with anti-ubiquitin (α-Ub) (**d**) or antibody specific for K48-linked ubiquitin (α-Ub(K48)) (**e**). (**f**) Immunoblot analysis of the co-immunoprecipitation of ectopic Xpress-tagged smARF and HA-Jnk2 in *Arf*$^{-/-}$ MEFs transfected to express Xpress-tagged smARF and/or HA-Jnk2 and treated with MG-132. (**g**) Immunoblot analysis of the co-immunoprecipitation of Xpress-tagged smARF and endogenous Jnk2 in untransfected wild-type MEFs (WT) or wild-type MEFs stably expressing Xpress-tagged smARF (WT^{smARF}), treated with MG-132. NS (top), nonspecific band. Data are representative of three independent experiments.

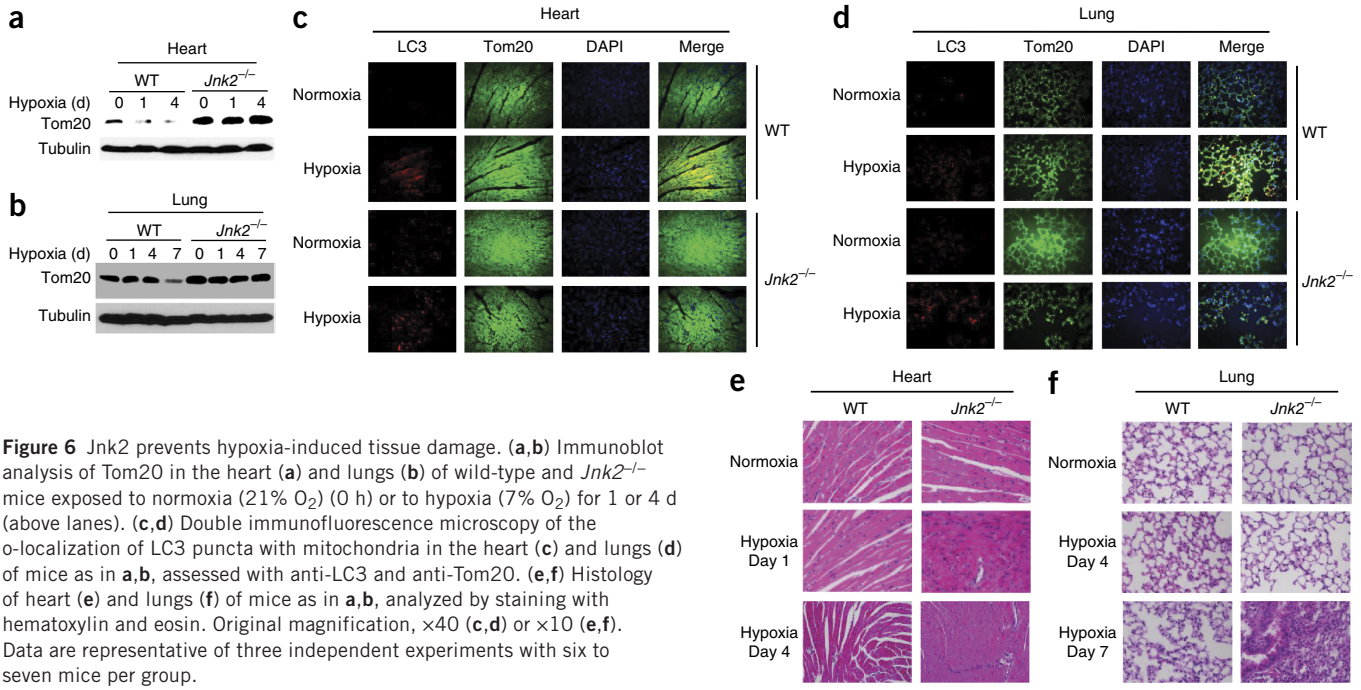

Figure 6 Jnk2 prevents hypoxia-induced tissue damage. (**a**,**b**) Immunoblot analysis of Tom20 in the heart (**a**) and lungs (**b**) of wild-type and *Jnk2*$^{-/-}$ mice exposed to normoxia (21% O_2) (0 h) or to hypoxia (7% O_2) for 1 or 4 d (above lanes). (**c**,**d**) Double immunofluorescence microscopy of the o-localization of LC3 puncta with mitochondria in the heart (**c**) and lungs (**d**) of mice as in **a**,**b**, assessed with anti-LC3 and anti-Tom20. (**e**,**f**) Histology of heart (**e**) and lungs (**f**) of mice as in **a**,**b**, analyzed by staining with hematoxylin and eosin. Original magnification, ×40 (**c**,**d**) or ×10 (**e**,**f**). Data are representative of three independent experiments with six to seven mice per group.

decreased the K48-linked polyubiquitination of smARF (**Fig. 5d**,**e**). Co-immunoprecipitation assays showed that smARF specifically interacted with ectopically expressed Jnk2 but not Jnk1 (**Fig. 5f** and **Supplementary Fig. 5d**), as well as with endogenous Jnk2 (**Fig. 5g**). Jnk2 partially localized in mitochondria, where smARF exclusively resides, at steady state (**Supplementary Fig. 5e**), which suggested that Jnk2 might target smARF for proteasomal degradation in the mitochondria. Although Jnk2 also interacted with full-length p19ARF (**Supplementary Fig. 5f**), it did not affect the ubiquitination of p19ARF (**Supplementary Fig. 5g**). Together these data suggested that Jnk2 facilitated K48-linked polyubiquitination of smARF to promote its proteasomal degradation.

Jnk2 prevents hypoxia-induced tissue damage

To understand the role of Jnk2 in stress-induced mitophagy, we used hypoxia as an *in vivo* model. We exposed wild-type and *Jnk2*$^{-/-}$ mice to normoxia (21% O_2) or hypoxia (7% O_2) for 1, 4 or 7 d. The expression of Tom20 protein gradually decreased in the heart and lungs of hypoxic wild-type mice (**Fig. 6a**,**b**). In contrast, the degradation of Tom20 was inhibited in the heart and lungs of hypoxic *Jnk2*$^{-/-}$ mice (**Fig. 6a**,**b**). Dual immunofluorescence staining of heart and lungs from hypoxic wild-type mice showed co-localization of LC3 puncta with mitochondria; this was substantially diminished in *Jnk2*$^{-/-}$ mice (**Fig. 6c**,**d**). Histology analysis revealed more obvious damage in the heart and lungs of hypoxic *Jnk2*$^{-/-}$ mice than in those of their wild-type counterparts (**Fig. 6e**,**f**). We also observed less p62 protein and more accumulation of smARF in the heart and lungs of *Jnk2*$^{-/-}$ mice than in those of wild-type mice at steady state (**Supplementary Fig. 6a**,**b**). Together these data indicated that Jnk2 functioned as a guardian to protect organs such as heart and lung from hypoxia-induced damage through the promotion of mitophagy.

Jnk2 suppresses activation of inflammasomes

Defective mitophagy has been reported to induce excessive mitochondrial ROS, which leads to the hyperactivation of inflammasomes and elaboration of mature interleukin 1β (IL-1β)[3–5]. To determine the role of Jnk2-mediated mitophagy in regulating the activation of inflammasomes, we isolated bone marrow–derived macrophages (BMDMs) from wild-type and *Jnk2*$^{-/-}$ mice, primed the cells with lipopolysaccharide (LPS) and then stimulated them with ATP to activate inflammasomes[5]. Under these conditions, *Jnk2*$^{-/-}$ BMDMs secreted significantly more IL-1β and IL-18, as well as active, cleaved caspase-1 and IL-1β, than did wild-type BMDMs (**Fig. 7a**,**b**). The enhanced inflammasome activity in the *Jnk2*$^{-/-}$ BMDMs was not the result of altered activation of upstream signaling molecules, including the transcription factor NF-κB and kinases p38 and Erk, as activation of these molecules was similar in wild-type and *Jnk2*$^{-/-}$ BMDMs (**Supplementary Fig. 7a**). Consistent with that, treatment with LPS plus ATP induced mitophagy in wild-type BMDMs but not in *Jnk2*$^{-/-}$ BMDMs, as shown by immunoblot analysis with anti-Tom20 and the colocalization of LC3 puncta with mitochondria (**Fig. 7c**,**d**). Under the same conditions, the amount of mitochondrial ROS in *Jnk2*$^{-/-}$ BMDMs was greater than that in wild-type BMDMs (**Fig. 7e**). Treatment with Mito-TEMPO, an antioxidant targeted to mitochondria that is a scavenger specific for mitochondrial ROS[5], abrogated the increase in the secretion of IL-1β and IL-18 in *Jnk2*$^{-/-}$ BMDMs in response to LPS plus ATP (**Fig. 7f**). Furthermore, ectopic expression of p62 inhibited the enhanced secretion of IL-1β and IL-18 in *Jnk2*$^{-/-}$ BMDMs in response to LPS and ATP (**Fig. 7g** and **Supplementary Fig. 7b**). The partial inhibition of the enhanced secretion of IL-1β and IL-18 in *Jnk2*$^{-/-}$ BMDMs by p62 was most probably due to the relatively low transduction efficiency of the p62-expressing lentivirus (~30%). Silencing of *Jnk2* in the mouse alveolar macrophage cell line MH-S also enhanced the secretion of IL-1β and IL-18 in response to LPS plus ATP (**Supplementary Fig. 7c**). Similarly, the addition of antimycin A or rotenone, which inhibit the mitochondrial respiratory complex I or complex III, respectively, induced more secretion of IL-1β and IL-18 and/or production of mitochondrial ROS in LPS-primed *Jnk2*$^{-/-}$ BMDMs than in their wild-type counterparts (**Supplementary Fig. 7d**,**e**).

To further determine the *in vivo* relevance of the regulation of inflammasome activation by Jnk2, we used an animal model of

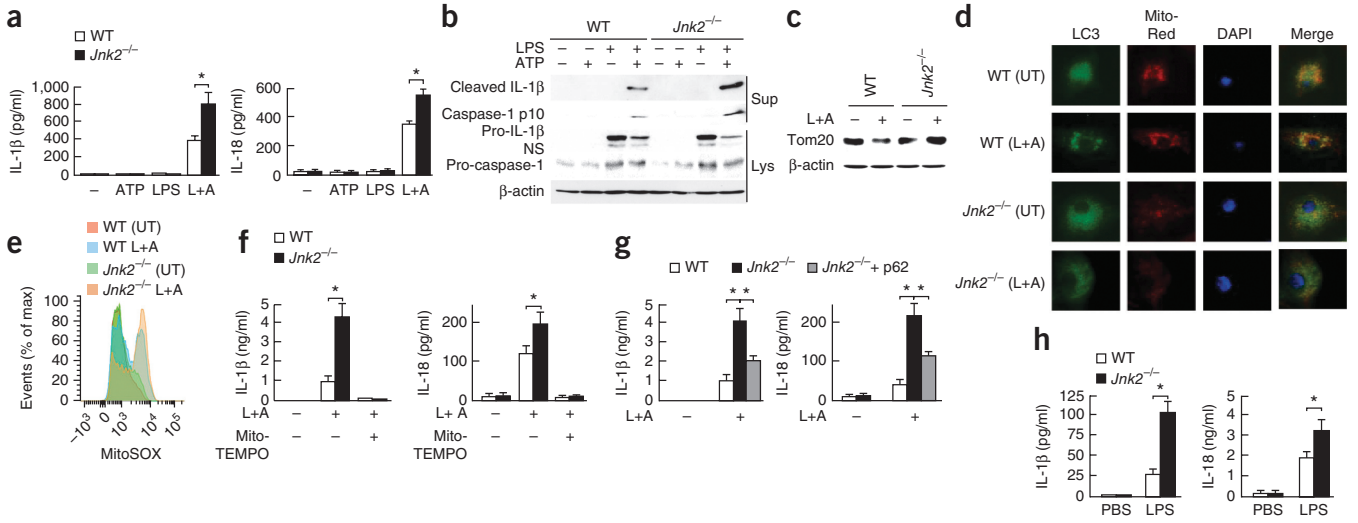

Figure 7 Loss of Jnk2 enhances the activation of inflammasomes. (**a**) Secretion of IL-1β and IL-18 from wild-type and *Jnk2*$^{-/-}$ BMDMs left untreated (–) or treated with LPS or ATP or both (L+A) (horizontal axes). (**b**) Immunoblot analysis of IL-1β and caspase-1 (p10 indicates cleavage) in wild-type and *Jnk2*$^{-/-}$ BMDMs treated as in **a** (above lanes). (**c**) Immunoblot analysis of the degradation of Tom20 in wild-type and *Jnk2*$^{-/-}$ BMDMs left untreated (–) or treated with LPS and ATP (+). (**d**) Microscopy of the co-localization of LC3 puncta with mitochondria in wild-type and *Jnk2*$^{-/-}$ BMDMs left untreated (UT) or treated with LPS and ATP (L+A). Original magnification, ×40. (**e**) Generation of mitochondrial ROS in wild-type and *Jnk2*$^{-/-}$ BMDMs treated as in **d**. (**f**) Secretion of IL-1β and IL-18 from wild-type and *Jnk2*$^{-/-}$ BMDMs given no pretreatment (–) or pretreated with Mito-TEMPO (+), followed by treatment as in **d**. (**g**) Secretion of IL-1β and IL-18 from wild-type and *Jnk2*$^{-/-}$ BMDMs transduced with control lentiviral vector or lentiviral vector encoding Xpress-tagged p62 (+ p62), then left untreated (–) or treated with LPS and ATP (+). (**h**,**i**) Serum IL-1β and IL-18 (**h**) and survival (**i**) of wild-type and *Jnk2*$^{-/-}$ mice given intraperitoneal injection of LPS (12 mg (**h**) or 34 mg (**i**) per kg body weight). $^{*}P < 0.05$ (unpaired Student's *t*-test (**a**,**f**–**h**)) or $P = 0.0106$ (log-rank test (**i**)). Data are representative of five (**a**) or three (**b**–**i**) independent experiments (mean and s.e.m. of three (**a**,**f**,**g**) or five to six (**h**) mice per group with technical duplicates, eight to nine mice per group (**i**) or three mice per group (**b**–**e**)).

endotoxic shock. Consistent with the *in vitro* results, serum concentrations of IL-1β and IL-18 were significantly higher in endotoxemic *Jnk2*$^{-/-}$ mice than in their wild-type counterparts (**Fig. 7h**). *Jnk2*$^{-/-}$ mice were more susceptible to LPS-induced mortality than were wild-type mice (**Fig. 7i**). *Jnk2*$^{-/-}$ BMDMs also had less p62 protein and more smARF protein at steady state than did wild-type BMDMs (**Supplementary Fig. 7f**). Together these data demonstrated that loss of Jnk2 resulted in the hyperactivation of inflammasomes.

Erythroid maturation does not require Jnk2

Mitophagy is critical for the coordinated removal of mitochondria during the terminal differentiation of erythrocytes. We found that red blood cell (RBC) counts and the concentration of hemoglobin and hematocrit in the peripheral blood were similar in wild-type mice and *Jnk2*$^{-/-}$ mice (**Supplementary Fig. 7g**). We also examined RBCs for expression of the erythroid cell marker Ter119 and the transferrin receptor CD71 (which is downregulated during terminal erythrocyte differentiation). The frequency of Ter119^{+}CD71^{+} reticulocytes and mature CD71^{-} erythrocytes in the blood was also similar in wild-type and *Jnk2*$^{-/-}$ mice (**Supplementary Fig. 7h**). In addition, there were similar populations of CD71^{-} RBCs negative for the mitochondrial stain MitoTracker Green, as well as CD71^{+} RBCs positive for MitoTracker Green, in wild-type and *Jnk2*$^{-/-}$ mice (**Supplementary Fig. 7i**). These data suggested that loss of Jnk2 did not affect erythrocyte differentiation at steady state, which indicated different roles for Jnk2 in mitophagy under stress and in developmental conditions.

DISCUSSION

Overwhelming evidence has shown a fundamental role for mitophagy in many physiological events, from development to aging, and its deregulation contributes to many diseases, including neurodegenerative diseases and immunological disorders[1–5]. Although a series of key components in the mitophagy machinery have been identified[6–8], how mitophagy is regulated has remained largely unknown. In this report, we demonstrated that Jnk2 was required for stress-induced mitophagy through the promotion of ubiquitination-dependent proteasomal degradation of smARF. Loss of Jnk2 resulted in tissue damage under hypoxic stress, as well as inflammasome hyperactivation and increased mortality in sepsis. Thus, Jnk2 functions as a guardian for organ integrity and thereby determines life or death under environmental stress.

Jnk2 positively regulated stress-induced mitophagy through targeting smARF for degradation independently of its kinase activity. It has been reported that Jnk1 is involved in starvation-induced autophagy through phosphorylation of Bcl-2 and inhibition of its association with beclin-1 (ref. 32). Our results have provided genetic evidence that Jnk2, but not Jnk1, targeted smARF for ubiquitination-dependent proteasomal degradation at steady state in a kinase activity–independent manner and thereby ensured that cells mounted efficient mitophagy to eliminate damaged mitochondria under stress *in vitro* and *in vivo*. Although the underlying mechanism by which Jnk2 targets smARF for ubiquitination has yet to be determined, our observation that Jnk2 interacted with smARF would suggest that Jnk2 might act as an adaptor to facilitate the interaction of smARF with its E3 ligase. The cellular compartment in which Jnk2 targets smARF for proteasomal degradation also remains to be determined. However, our results showed that Jnk2 localized to the mitochondria, where smARF exclusively resides. Therefore, it is possible that Jnk2 might target smARF for proteasomal degradation in mitochondria. Although Jnk2 also interacted with full-length p19ARF, it did not affect the ubiquitination of p19ARF. It is possible that the amino-terminal region of p19ARF,

which mediates its binding to many cofactors but is not present in smARF[38,39], may interfere with Jnk2-mediated ubiquitination of p19ARF. Although p19ARF contributes to autophagy when overexpressed or under pathological conditions such as oncogenic stress or in cancer cells[22,40,41], the slightly increased abundance of p19ARF in *Jnk2*$^{-/-}$ cells is less likely to have been accountable for the enhanced autophagy and decreased p62 expression at steady state, as complementation of *Arf*$^{-/-}$ cells with mutant ARF that generated only full-length p19ARF did not reduce the steady-state abundance of p62. Thus, smARF might have had a dominant role in the enhanced autophagy in Jnk2-deficient cells.

The ubiquitin- and LC3-binding adaptor p62 was essential for the promotion of stress-induced mitophagy by Jnk2. The role of p62 in mitophagy has been controversial. While it has been reported that p62 is critical for the removal of depolarized mitochondria via mitophagy[1,2,6,8,11–16], it has also been shown that p62 is dispensable for mitophagy, possibly due to the redundancy with the related ubiquitin- and LC3-binding protein NBR1 (refs. 2,42). Our results showed that loss of Jnk2 enhanced the lysosomal degradation of steady-state p62, which resulted in defective mitophagy upon stress, while ectopic expression of p62 in *Jnk2*$^{-/-}$ MEFs restored mitophagy in response to stress. Consistent with that, silencing of the gene encoding p62 resulted in defective mitophagy upon cellular stress. Thus, our studies demonstrated a crucial role for p62 in the Jnk2-mediated regulation of mitophagy upon stress.

smARF has a dual function in autophagy and mitophagy. Published studies have shown that ectopic overexpression of smARF is able to induce mitochondrial depolarization and autophagy and/or mitophagy[19]. However, the pathophysiological function of endogenous smARF is not known. Our results showed that loss of Jnk2 induced the accumulation of smARF, which resulted in more steady-state autophagy in unstimulated cells, consistent with published results obtained by ectopic overexpression of smARF[19]. Paradoxically, our results revealed that accumulated endogenous smARF in the absence of Jnk2 enhanced the steady-state autophagy that caused more lysosomal degradation of p62, which resulted in defective stress-induced mitophagy. Thus, the endogenous smARF that accumulated in the absence of Jnk2 regulated autophagy and mitophagy by two distinct but interrelated mechanisms: promotion of steady-state autophagy and suppression of stress-induced mitophagy.

We observed slightly more Tom20 protein at baseline in Jnk2-deficient cells, which was not 'rescued' by overexpression of p62. In addition, silencing of *Jnk2* in *Arf*$^{-/-}$ MEFs still resulted in more Tom20 without a decrease in the abundance of p62 at steady state. In contrast, either ectopic expression of p62 or silencing of the gene encoding smARF restored the degradation of Tom20 in Jnk2-deficient cells in response to inducers of mitophagy, regardless of the basal amount of Tom20. Moreover, in *Arf*$^{-/-}$ MEFs, the stress-induced degradation of Tom20 and steady-state expression of p62 were not affected by silencing of *Jnk2*, although an increase in the basal abundance of Tom20 was caused by the knockdown of Jnk2 in these cells. Therefore, Jnk2 regulated stress-induced mitophagy via the smARF-p62 axis. It is likely that Jnk2 regulates basal Tom20 expression through a different mechanism, but this regulation is probably not involved in the regulation of stress-induced mitophagy by Jnk2.

Jnk2 is not required for erythroid maturation. It is known that mitophagy is critical for the elimination of mitochondria during erythroid maturation[43]. Our finding that Jnk2 was critical for mitophagy under stress conditions but not during erythroid maturation indicated that Jnk2 regulates mitophagy differently under stress conditions and developmental conditions. During reticulocyte maturation, it is possible that either Jnk2-maintained p62 is not required for this type of mitophagy or that its deficiency is compensated by other pathways, such as that of Nix, a mitochondrial protein that is able to directly bind to LC3 and whose expression substantially upregulated during terminal erythroid differentiation[43].

Our findings have identified Jnk2 as a previously unknown key regulator of inflammasome activation. Our results showed that *Jnk2*$^{-/-}$ BMDMs, which had defective stress-induced mitophagy and excessive ROS, had increased secretion of IL-1β and IL-18, as well as active caspase-1 and IL-1β, in response to LPS and ATP. More notably, *Jnk2*$^{-/-}$ mice had increased concentrations of serum IL-1β and IL-18 and higher mortality rate, accompanied by impaired clearance of damaged mitochondria, compared with that of wild-type mice, in a mouse model of sepsis. Thus, the promotion of stress-activated mitophagy by Jnk2 might have a critical role in preventing the hyperactivation of inflammasomes. Sepsis represents an exaggerated systemic inflammatory response to infection that can progress to multi-organ failure, including shock[44,45]. So far there is no effective treatment for sepsis. It has long been considered that sepsis is a condition associated with mitochondrial dysfunction, and a study of the metabolome and proteome in septic patients has revealed that mitochondrial dysfunction can serve as a signature indicative of the outcome of sepsis[46]. In support of that observation, a published report has shown that upregulation of autophagy not only inhibits inflammatory cytokine production but also confers tissue tolerance to damage in sepsis, which might represent an efficacious therapeutic option for sepsis[47,48]. Thus, the promotion of mitophagy by Jnk2 might protect organs from sepsis-induced damage by at least two interrelated mechanisms: by suppressing inflammasome activation, and by conferring tissue tolerance to damage. Targeting both inflammation and tissue tolerance to damage by upregulating mitophagy may be critical to the prevention of sepsis-induced tissue damage and organ failure. It will be of interest to investigate whether Jnk2 is dysregulated during sepsis in mice. Furthermore, targeting Jnk2-regulated mitophagy for tissue tolerance to damage may have broad applications to many other pathological conditions that, like sepsis, are associated with mitochondrial dysfunction.

METHODS

Methods and any associated references are available in the online version of the paper.

Note: Any Supplementary Information and Source Data files are available in the online version of the paper.

ACKNOWLEDGMENTS

We thank M. Karin (University of California, San Diego) for *Jnk2*$^{-/-}$ mice; R. Youle (National Institute of Neurological Disorders and Stroke, National Institutes of Health) for the mCherry-parkin plasmid; Y. Cheng and M.A. Baker for help with the analysis of inflammasome activation; A. Yemelyanov for lentivirus preparation; and J. Hou for help with animal work. Supported by the US National Institutes of Health (HL114763 to J.L.) and the American Asthma Foundation (13-0114 to J.L.).

AUTHOR CONTRIBUTIONS

Q.Z. and H.K. did experiments and analyzed the data; C.C., J.Y. and H.C.D.-U. did experiments; X.L., L.D., K.M.R. and N.S.C. provided reagents; and J.L. designed and supervised the study, did experiments, analyzed the data and wrote the manuscript.

COMPETING FINANCIAL INTERESTS

The authors declare no competing financial interests.

1. Youle, R.J. & Narendra, D.P. Mechanisms of mitophagy. *Nat. Rev. Mol. Cell Biol.* **12**, 9–14 (2011).

2. Ding, W.X. & Yin, X.M. Mitophagy: mechanisms, pathophysiological roles, and analysis. *Biol. Chem.* **393**, 547–564 (2012).
3. Lupfer, C. *et al.* Receptor interacting protein kinase 2-mediated mitophagy regulates inflammasome activation during virus infection. *Nat. Immunol.* **14**, 480–488 (2013).
4. Zhou, R., Yazdi, A.S., Menu, P. & Tschopp, J. A role for mitochondria in NLRP3 inflammasome activation. *Nature* **469**, 221–225 (2011).
5. Nakahira, K. *et al.* Autophagy proteins regulate innate immune responses by inhibiting the release of mitochondrial DNA mediated by the NALP3 inflammasome. *Nat. Immunol.* **12**, 222–230 (2011).
6. Hollville, E., Carroll, R.G., Cullen, S.P. & Martin, S.J. Bcl-2 family proteins participate in mitochondrial quality control by regulating Parkin/PINK1-dependent mitophagy. *Mol. Cell* **55**, 451–466 (2014).
7. Hasson, S.A. *et al.* High-content genome-wide RNAi screens identify regulators of parkin upstream of mitophagy. *Nature* **504**, 291–295 (2013).
8. Geisler, S. *et al.* PINK1/Parkin-mediated mitophagy is dependent on VDAC1 and p62/SQSTM1. *Nat. Cell Biol.* **12**, 119–131 (2010).
9. Koyano, F. *et al.* Ubiquitin is phosphorylated by PINK1 to activate parkin. *Nature* **510**, 162–166 (2014).
10. Moscat, J. & Diaz-Meco, M.T. p62 at the crossroads of autophagy, apoptosis, and cancer. *Cell* **137**, 1001–1004 (2009).
11. Lee, J.Y., Nagano, Y., Taylor, J.P., Lim, K.L. & Yao, T.P. Disease-causing mutations in parkin impair mitochondrial ubiquitination, aggregation, and HDAC6-dependent mitophagy. *J. Cell Biol.* **189**, 671–679 (2010).
12. Okatsu, K. *et al.* p62/SQSTM1 cooperates with Parkin for perinuclear clustering of depolarized mitochondria. *Genes Cells* **15**, 887–900 (2010).
13. Ding, W.X. *et al.* Nix is critical to two distinct phases of mitophagy, reactive oxygen species-mediated autophagy induction and Parkin-ubiquitin-p62-mediated mitochondrial priming. *J. Biol. Chem.* **285**, 27879–27890 (2010).
14. Politi, Y. *et al.* Paternal mitochondrial destruction after fertilization is mediated by a common endocytic and autophagic pathway in *Drosophila*. *Dev. Cell* **29**, 305–320 (2014).
15. Geisler, S., Vollmer, S., Golombek, S. & Kahle, P.J. The ubiquitin-conjugating enzymes UBE2N, UBE2L3 and UBE2D2/3 are essential for Parkin-dependent mitophagy. *J. Cell Sci.* **127**, 3280–3293 (2014).
16. Park, S., Choi, S.G., Yoo, S.M., Son, J.H. & Jung, Y.K. Choline dehydrogenase interacts with SQSTM1/p62 to recruit LC3 and stimulate mitophagy. *Autophagy* **10**, 1906–1920 (2014).
17. Kirkin, V., McEwan, D.G., Novak, I. & Dikic, I. A role for ubiquitin in selective autophagy. *Mol. Cell* **34**, 259–269 (2009).
18. Sahani, M.H., Itakura, E. & Mizushima, N. Expression of the autophagy substrate SQSTM1/p62 is restored during prolonged starvation depending on transcriptional upregulation and autophagy-derived amino acids. *Autophagy* **10**, 431–441 (2014).
19. Reef, S. *et al.* A short mitochondrial form of p19ARF induces autophagy and caspase-independent cell death. *Mol. Cell* **22**, 463–475 (2006).
20. Reef, S. & Kimchi, A. Nucleolar p19ARF, unlike mitochondrial smARF, is incapable of inducing p53-independent autophagy. *Autophagy* **4**, 866–869 (2008).
21. Budina-Kolomets, A., Hontz, R.D., Pimkina, J. & Murphy, M.E. A conserved domain in exon 2 coding for the human and murine ARF tumor suppressor protein is required for autophagy induction. *Autophagy* **9**, 1553–1565 (2013).
22. Abida, W.M. & Gu, W. p53-Dependent and p53-independent activation of autophagy by ARF. *Cancer Res.* **68**, 352–357 (2008).
23. Hibi, M., Lin, A., Smeal, T., Minden, A. & Karin, M. Identification of an oncoprotein- and UV-responsive protein kinase that binds and potentiates the c-Jun activation domain. *Genes Dev.* **7**, 2135–2148 (1993).
24. Chang, L. & Karin, M. Mammalian MAP kinase signalling cascades. *Nature* **410**, 37–40 (2001).
25. Davis, R.J. Signal transduction by the JNK group of MAP kinases. *Cell* **103**, 239–252 (2000).
26. Liu, J., Minemoto, Y. & Lin, A. c-Jun N-terminal protein kinase 1 (JNK1), but not JNK2, is essential for tumor necrosis factor α-induced c-Jun kinase activation and apoptosis. *Mol. Cell. Biol.* **24**, 10844–10856 (2004).
27. Sabapathy, K. *et al.* Distinct roles for JNK1 and JNK2 in regulating JNK activity and c-Jun-dependent cell proliferation. *Mol. Cell* **15**, 713–725 (2004).
28. Fuchs, S.Y., Dolan, L., Davis, R.J. & Ronai, Z. Phosphorylation-dependent targeting of c-Jun ubiquitination by Jun N-kinase. *Oncogene* **13**, 1531–1535 (1996).
29. Fuchs, S.Y. *et al.* c-Jun NH2-terminal kinases target the ubiquitination of their associated transcription factors. *J. Biol. Chem.* **272**, 32163–32168 (1997).
30. Fuchs, S.Y., Fried, V.A. & Ronai, Z. Stress-activated kinases regulate protein stability. *Oncogene* **17**, 1483–1490 (1998).
31. Fuchs, S.Y. *et al.* JNK targets p53 ubiquitination and degradation in nonstressed cells. *Genes Dev.* **12**, 2658–2663 (1998).
32. Wei, Y., Pattingre, S., Sinha, S., Bassik, M. & Levine, B. JNK1-mediated phosphorylation of Bcl-2 regulates starvation-induced autophagy. *Mol. Cell* **30**, 678–688 (2008).
33. Wu, W. *et al.* ULK1 translocates to mitochondria and phosphorylates FUNDC1 to regulate mitophagy. *EMBO Rep.* **15**, 566–575 (2014).
34. Liu, L. *et al.* Mitochondrial outer-membrane protein FUNDC1 mediates hypoxia-induced mitophagy in mammalian cells. *Nat. Cell Biol.* **14**, 177–185 (2012).
35. Guo, J.Y. *et al.* Activated Ras requires autophagy to maintain oxidative metabolism and tumorigenesis. *Genes Dev.* **25**, 460–470 (2011).
36. Bianchi, M.E. Killing cancer cells, twice with one shot. *Cell Death Differ.* **21**, 1–2 (2014).
37. Li, N. *et al.* Loss of acinar cell IKKα triggers spontaneous pancreatitis in mice. *J. Clin. Invest.* **123**, 2231–2243 (2013).
38. Kuo, M.L., den Besten, W., Bertwistle, D., Roussel, M.F. & Sherr, C.J. N-terminal polyubiquitination and degradation of the Arf tumor suppressor. *Genes Dev.* **18**, 1862–1874 (2004).
39. Chen, D., Shan, J., Zhu, W.G., Qin, J. & Gu, W. Transcription-independent ARF regulation in oncogenic stress-mediated p53 responses. *Nature* **464**, 624–627 (2010).
40. Pimkina, J. & Murphy, M.E. ARF, autophagy and tumor suppression. *Autophagy* **5**, 397–399 (2009).
41. Balaburski, G.M., Hontz, R.D. & Murphy, M.E. p53 and ARF: unexpected players in autophagy. *Trends Cell Biol.* **20**, 363–369 (2010).
42. Narendra, D., Kane, L.A., Hauser, D.N., Fearnley, I.M. & Youle, R.J. p62/SQSTM1 is required for Parkin-induced mitochondrial clustering but not mitophagy; VDAC1 is dispensable for both. *Autophagy* **6**, 1090–1106 (2010).
43. Sandoval, H. *et al.* Essential role for Nix in autophagic maturation of erythroid cells. *Nature* **454**, 232–235 (2008).
44. Hotchkiss, R.S. & Karl, I.E. The pathophysiology and treatment of sepsis. *N. Engl. J. Med.* **348**, 138–150 (2003).
45. Angus, D.C. & van der Poll, T. Severe sepsis and septic shock. *N. Engl. J. Med.* **369**, 840–851 (2013).
46. Langley, R.J. *et al.* An integrated clinico-metabolomic model improves prediction of death in sepsis. *Sci. Transl. Med.* **5**, 195ra195 (2013).
47. Figueiredo, N. *et al.* Anthracyclines induce DNA damage response-mediated protection against severe sepsis. *Immunity* **39**, 874–884 (2013).
48. Medzhitov, R. Septic shock: on the importance of being tolerant. *Immunity* **39**, 799–800 (2013).

ONLINE METHODS

Mice. *Jnk2*$^{-/-}$ mice on the C57BL/6 background were provided by M. Karin. The animal care and experiments were performed in compliance with the institutional and US National Institutes of Health guidelines and were approved by the Northwestern University Animal Care and Use Committee. For the mortality studies, when mice became moribund (hunched posture, lack of curiosity, little or no response to stimuli and not moving when touched), a clinically irreversible condition that leads to inevitable death, according to the guidelines for the selection of humane endpoints in rodent studies at Northwestern University, they were killed.

MEFs and treatment. Jnk1- or Jnk2-deficient MEFs have been described[26]. Cells were exposed to normoxia (21% O_2) or hypoxia (1.5% O_2) or were treated with CCCP (10 μM) or were starved by incubation in HBSS.

Reagents. Tumor-necrosis factor was from R&D Systems. LPS (L2630), antimycin A, CCCP, rotenone, Mito-TEMPO, bafilomycin A1, MG-132 and cycloheximide were from Sigma-Aldrich. ATP was from ENZO Life Sciences. TMRE, MitoTracker Deep Red, MitoTracker Green and MitoSox Red were from Life Technologies. HBSS was from CellGro. The ProcartaPlex Mouse Basic kit, mouse IL-1β Simplex and IL-18 Simplex were from eBioscience. Monoclonal antibodies used in this study are listed in **Supplementary Table 1**. The mCherry-parkin plasmid was a gift from R. Youle (plasmid 23956; Addgene)[1,2]. The following siRNA oligonucleotides were from Thermo Scientific (Dharmacon products): control siRNA (D-001210-02); *Arf*-specific siRNA 1 (5′-AGGUGAUGAUGAUGGGCAATT-3′); *Arf*-specific siRNA 2 (5′-GGUCGCAGGUUCUUGGUCATT-3′); siRNA specific for the gene encoding p62 (L-047628-01); Jnk2-specific siRNA (5′-CCGCAGAGUUCAUGAAGAATT-3′); *Jnk1*-specific siRNA (5′-UGAUUCAGAUGGAGUUAGATT-3′); siRNA specific for the gene encoding beclin-1 (5′-CAGUUUGGCACAAUCAAUATT-3′); and *Atg5*-specific siRNA (5′-CAUCAACCGGAAACUCAUTT-3′).

Lentivirus infection. Cells (3×10^5) were infected with 0.5 ml lentivirus stock (1×10^7 to 1×10^8 transduction units per ml) twice every 6 h. Cells were washed once between the infections by the addition of cell culture medium for 30 min, as described[49].

***In vivo* experiments.** For hypoxic mouse model, female wild-type or *Jnk2*$^{-/-}$ mice (6–8 weeks of age) were exposed to normoxia (21% O_2) or hypoxia (7% O_2) for 1, 4 or 7 d. Heart and lungs from a subgroup of mice were collected and the homogenates were lysed in RIPA buffer (50 mM Tris HCl pH7.4, 150 mM NaCl, 2 mM EDTA, 0.5% sodium deoxycholate, 1% NP-40 and 0.1% SDS) to prepare protein extracts for immunoblot analysis. For another subgroup of mice, heart and lung tissues were fixed, embedded in paraffin and analyzed by staining with hematoxylin and eosin. For mouse model of sepsis, mice were given intraperitoneal injection of *Escherichia coli* LPS (12 mg per kg body weight; or 34 mg per kg body weight, for mortality studies).

Analysis of cytokines. The concentrations of cytokines, including IL-1β and IL-18, in the cell culture supernatants or mouse serum were determined by multiplex immunoassay (eBioscience).

Isolation and culture of mouse BMDMs. BMDMs were isolated as described[50]. Bone marrow cells collected from mouse femurs were plated on Petri dishes and were cultured for 5 d in DMEM containing 10% FBS with 2 mM L-glutamine, 100 units/ml penicillin, 100 μg/ml streptomycin and 25% medium conditioned with L929 mouse fibroblasts.

Analysis of inflammasome activation. Cells were primed for 16 h with LPS (10 ng/ml), followed by treatment for 1 h with ATP (2 mM) or for 6 h with rotenone (40 μM) or antimycin A (10 μg/ml). Supernatants were collected for cytokine analysis or proteins were precipitated from the supernatants for immunoblot analysis with anti-caspase-1 or anti-IL-1β (**Supplementary Table 1**). Cells were lysed for immunoblot analysis with anti-caspase-1 or anti-IL-1β (**Supplementary Table 1**). In some experiments, cells were pretreated with Mito-TEMPO (200 μM) for 1 h before treatment with LPS and ATP.

Measurement of mitochondrial ROS. Cells were stained for 15 min at 37 °C with MitoSOX (5 μM). Cells were then washed with PBS, detached by treatment with trypsin and suspended in PBS containing 1% FBS. Data were acquired with a BD LSRFortessa Analyzer and were analyzed with FlowJo analytical software (TreeStar).

Transmission electron microscopy. Cells were fixed in 4% formaldehyde and 1% glutaraldehyde and then were processed for transmission electron microscopy by the Northwestern University Cell Imaging Facility.

Generation of stable cell lines and siRNA transfection. Wild-type or *Jnk2*$^{-/-}$ MEFs were transfected with pEGFP-LC3 vector encoding GFP-LC3 or pcDNA3.1 vector encoding Xpress-tagged smARF. 2 d after the transfection, cells were selected through the use of the aminoglycoside G418 (300 μg/ml). For siRNA transfection, cells were transfected with 100 nM siRNA.

Fluorescence microscopy. Cells stably expressing GFP-LC3 were incubated for 30 min at 37 °C with MitoTracker Deep Red (100 nM) and then were fixed with ice-cold methanol and mounted in solution containing DAPI (4,6-diamidino-2-phenylindole), followed by fluorescence microscopy. In some experiments, cells were incubated with MitoTracker Deep Red and then were fixed and permeabilized by subsequent incubations in ice-cold methanol and 0.02% NP40. Cells were then subjected to immunofluorescence staining with anti-Tom20 or anti-LC3 (**Supplementary Table 1**). For immunofluorescence staining of tissues, paraffin-embedded sections were deparaffinized and processed for double immunofluorescence staining with anti-Tom20 or anti-LC3 (**Supplementary Table 1**), by the Northwestern University Pathology Core Facility.

Cell fractionation. Cells were fractionated into cytoplasmic (cytosolic and mitochondrial) and nuclear fractions with a NE-PER Nuclear and Cytoplasmic Extraction Kit (Thermo Scientific) or were fractionated into cytosolic and mitochondrial fractions with a Mitochondria/Cytosol Fractionation Kit (BioVision), each used according to the manufacturer's instructions.

Mass spectrometry. Mass spectrometry analysis was done by K. Stone at the Mass Spectrometry Core Facility at Yale University.

Flow cytometry. Erythroid cells from peripheral blood were labeled for 30 min at 37 °C with 50 nM Mitotracker Green. The cells were then stained with phycoerythrin-conjugated anti-Ter119 (**Supplementary Table 1**) and allophycocyanin-conjugated anti-CD71 (**Supplementary Table 1**), followed by flow cytometry.

Statistical analysis. Data were analyzed by an unpaired Student's *t*-test or log-rank test, with the assumption of normal distribution of data and equal sample variance. Sample sizes were selected on the basis of preliminary results to ensure an adequate power. All cells and mice used for the study were included for the statistical analysis, with no randomization or blinding involved. No exclusion of data points was used.

49. Do-Umehara, H.C. *et al.* Suppression of inflammation and acute lung injury by Miz1 via repression of C/EBP-δ. *Nat. Immunol.* **14**, 461–469 (2013).
50. Liu, J. *et al.* Site-specific ubiquitination is required for relieving the transcription factor Miz1-mediated suppression on TNF-α-induced JNK activation and inflammation. *Proc. Natl. Acad. Sci. USA* **109**, 191–196 (2012).

doi:10.1038/ni.3130